Tree Physiology, 2025, tpaf051
https://doi.org/10.1093/treephys/tpaf051
Advance access publication date 25 April 2025
Research paper

Fiber-specific expression of *PdCel9A6* modifies the characteristics of wood fibers in *Populus*

Jian Li[1,†], Xulei Guo[2,†], Xianwen Lu[2], Jiayan Sun[3], Yongcan Jin[4], Meng Li[1,*] and Laigeng Li[3,*]

[1]Yuelushan Laboratory, College of Life Science and Technology, Central South University of Forestry and Technology, Shaoshan South Road, Tianxin District, Changsha, Hunan 410004, China
[2]Key Laboratory of Biodiversity Conservation in Southwest, State Forestry Administration, Southwest Forestry University, Bailong Temple, Panlong District, Kunming 650224, China
[3]Key Laboratory of Plant Carbon Capture, CAS Center for Excellence in Molecular Plant Sciences, Chinese Academy of Sciences, Fenglin Road, Xuhui District, Shanghai 200032, China
[4]Jiangsu Province Key Laboratory of Pulp and Paper Science and Technology, College of Light Industry and Food Engineering, Longpan Road, Xuanwu District, Nanjing Forestry University, Nanjing 210037, China

*Corresponding authors (limeng0422@csuft.edu.cn; lgli@cemps.ac.cn)

†Jian Li and Xulei Guo contributed equally.

Handling Editor: Heather Coleman

Wood fiber has been extensively used in the pulp and papermaking industries. The length of fiber cells is critical in determining the quality of paper. In our previous studies, we identified *PdCel9A6*, a gene encoding endo-1,4-β-glucanases expressed in the developing xylem to affect cell wall formation. In this study, we modified the *PdCel9A6* expression specifically in xylem fiber cells. The results showed that the fiber-specific upregulation of *PdCel9A6* resulted in increased plant height and internode length. The transgenics significantly increased the fiber cell length in the wood xylem. In wood cell wall components, the transgenics showed a reduction of lignin while increasing cellulose. Furthermore, the characteristics of the paper processed from the transgenics showed a significant improvement in paper strength. Transcriptome studies showed that upregulation of *PdCel9A6* in fiber cells leads to changes in transcription related to cell wall remodeling and thickening during xylem development. Together, the study demonstrated a new strategy of fiber cell wall modification that could have the potential to improve forest trees for better pulping and papermaking.

Keywords: cell expansion, endo-1,4-β-glucanase, pulping, wood formation, xylem fiber.

Introduction

Wood is an important renewable resource in the papermaking, furniture, construction, decoration and other industries. Wood in hardwood species is made up of vessel, fiber and ray cells that are differentiated from the proliferating cells of the vascular cambium (Luo and Li 2022, Zhu and Li 2024). Fiber cells are a major component of wood cells in hardwood species, accounting for the major part of pulping and papermaking products, and their length is vital to paper quality (Pulkkinen et al. 2006, Gharehkhani et al. 2015, Larsson et al. 2018).

Following cell division in the vascular cambium, fiber cells undergo cell elongation, cell wall biosynthesis and thickening, resulting in the development of mature fiber cells in wood (Zhu and Li 2024). This process is regulated by a series of genes involved in phytohormone signaling and cell wall formation, which influences the properties of wood fiber cells (Li et al. 2024, Zhu and Li 2024). In wood formation, auxin signaling plays a crucial role in regulating the development of wood fibers (Guo et al. 2024, Liu et al. 2025). In *Populus*, overexpressing an Arabidopsis gene, *AtGA20ox1*, for gibberellin biosynthesis results in longer xylem fibers (Eriksson et al. 2000). Brassinosteroids also play a role in regulating fiber elongation. The transcription factor *PagBEE3L* expression is induced by brassinosteroid to promote cell expansion in xylem. Overexpression of *PagBEE3L* causes an increase in stem diameter, xylem width and internode length in *Populus* (Noh et al. 2015). Multiple molecular networks are engaged in regulating fiber cell length during wood production.

Endo-1,4-β-glucanase (EGase, EC 3.2.1.4) hydrolyzes 1,4-β-D-glucan chain molecules and plays a pivotal role in various physiological processes (Yu et al. 2014, 2018, Linton 2020). Plants contain a large family of EGase genes that are involved in cellulose deposition related to growth and development, fruit ripening and organ shedding (Maloney et al. 2012, Linton 2020). As plant cells grow, EGases help facilitate the loosening of the cell wall by hydrolyzing non-crystallized cellulose, allowing for cell expansion and elongation (Park et al. 2003, Du et al. 2015). Overexpression of *PtrCel9A6* in *Arabidopsis* causes enlargement of leaf cells, fiber cells and xylem cells (Yu et al. 2013). The EGase mutant *Osglu3-1* of rice showed decreased root cell elongation rate and decreased meristem (J.W.Zhang et al. 2012).

The *Populus* genome has 27 EGase genes, which can be categorized into α, β and γ subfamilies, and each subfamily gene exhibits distinct effects on plant growth and development (Urbanowicz et al. 2007*a*, 2007*b*, Yu et al. 2013, Yu et al. 2014, Du et al. 2015). The α-subfamily EGase members *PtrGHB1*, *PtrGHB2* and *PtrGHB3* are mainly expressed in mature xylem; *PtrGHB4* is mainly expressed in developing xylem and mature leaves, and *PtrGHB5* and *PtrGHB13* are mainly expressed in the apical meristem (Du et al. 2015).

Received: January 17, 2025. **Revised:** April 2, 2025. **Accepted:** April 17, 2025

Additionally, *PopCel1* and *PopCel2* are two EGase genes in the *Populus* α-subfamily that are involved in leaf growth, and overexpression of these two genes promotes growth by enhancing cell expansion (Ohmiya et al. 2003, Park et al. 2003). The β subfamily comprises three members, including *PtrCel9A6*, *PtrGH9A7* and *PtrGH9A8*. *PtrCel9A6* is specifically expressed in developing xylem cells during secondary growth, and downregulation of *PtrCel9A6* expression causes secondary cell wall defects and xylem cellulose content reduction (Yu et al. 2013). Plant growth and biomass accumulation were significantly promoted by *PtrCel9A6* overexpression in *Arabidopsis thaliana*, while male sterility was caused by defects in anther dehiscence (Yu et al. 2013). *PtrGH9A7* and *PtrCel9A6* are a pair of genes that share a unique expression pattern. *PtrGH9A7* is mostly expressed in root tips, lateral root primordium, young leaves and cortex, although it is almost not expressed in the xylem. Notably, the expression of *PtrGH9A7* is significantly induced by auxin. Overexpression of *PtrGH9A7* leads to the expansion of leaf cells and root tip cells, resulting in enlarged leaves and increased root length (Yu et al. 2018). The γ subfamily comprises five members, namely *PtrKOR1*, *PtrKOR2*, *PtrCel9A3*, *PtrCel9A4* and *PtrCel9A5*. *PtrKOR1* exhibits abundant expression in the xylem tissue. Meanwhile, *PtrKOR2* and *PtrKOR5* are highly expressed in leaves, veins and petioles, and *PtrKOR3* and *PtrKOR4* are observed with their primary expression in the root. The down-regulation of *PtrKOR1* leads to a significant decrease in mechanical strength and defects in xylem development, resulting in reduced secondary wall thickness of vessel and fiber cells, along with decreased cellulose content (Yu et al. 2014). *Populus PtrKOR1* has been shown to be able to compensate for the phenotypic deficiency of the *kor1-1* mutant (Junko et al. 2009). Additionally, overexpression of *Populus KOR1* in *Eucalyptus tereticornis* resulted in a significant increase in cellulose content (Aggarwal et al. 2015). These findings collectively suggest that *PtrKOR1* plays a specific role in the regulation of cell wall biosynthesis.

In this study, we attempted to genetically modify the cell wall properties, particularly in fiber cells, by overexpressing *PdCel9A6* under the control of the fiber-specific promoters (Cao et al. 2020, Gui et al. 2020). The transgenics exhibited an increase in wood fiber length and changes in their wall property. The processed paper from the transgenics showed a significant improvement in mechanical strength. The study opens an avenue to genetically engineer wood properties for better paper production.

Materials and methods

Plant growth conditions

The *Populus* tree (*Populus deltoides* × *P. euramericana* cv. *Nanlin895*) was utilized in this study. The transgenics were grown in a phytotron with a light/dark cycle of 14/10 h, 60% relative humidity and a temperature of 25 °C. In field tests, the transgenics were planted in the Crop Cultivation and Breeding Station, Shanghai Institute of Plant Physiology and Ecology (39.937128° N, 121.122304° E).

Constructs and transformation

About 2 kb of the *DUF579-9* (Potri.005G141300) (Song et al. 2014) promoter *PdDUF579-9p* and 2 kb of the *WND1B* (Potri.001G448400) (Zhao et al. 2014) promoter *PdWND1Bp* were cloned from *P. deltoides* × *P. euramericana* cv. Nanlin895 (Cao et al. 2020, Gui et al. 2020). For cell-type-specific expression, the *Cel9A6* (Potri.005G237700) complementary DNA was cloned from *P. deltoides* × *P. euramericana* cv. 'Nanlin895' (*Pd*) and inserted into the vectors *pCAMBIA2300:PdDUF579-9p-35S mini-GUS* and *pCAMBIA2300: PdWND1Bp-35S mini-GUS* to obtain the constructs *pCAMBIA2300:PdDUF579-9p-35S mini-PdCel9A6* and *pCAMBIA2300:PdWND1Bp-35Smini-PdCel9A6*, respectively. The constructed *pCAMBIA2300:PdDUF579-9p-35S mini-PdCel9A6* and *pCAMBIA2300:PdWND1Bp-35Smini-PdCel9A6* vectors were transferred into the *Agrobacterium* strain GV3101 for genetic transformation according to the procedure (Li et al. 2003, 2005). Primers used for vector construction are listed in Table S1 available as Supplementary Data at *Tree Physiology* Online.

Quantitative reverse transcription-PCR and western blot assays

Total RNA was specifically isolated from the xylem tissues of the 12th–15th internodes using a total RNA extraction kit, following the manufacturer's instructions (Omega, R6827-02). The first-strand cDNA was synthesized from the total RNA using cDNA Synthesis SuperMix (TransGen, AT311-03) and utilized for the RT-PCR analysis of gene expression with gene-specific primers (see Table S1, available as Supplementary Data at *Tree Physiology* Online). RT-PCR was conducted using PerfectStart Green qPCR SuperMix (TransGen, AQ601) and a QuantStudio 3 Real-Time PCR Detection System (Thermo Fisher Scientific) following the manufacturer's protocol. *PdActin2* (Potri.001G309500) was employed as an internal control for normalizing target gene expression in each sample.

To analyze PdCel9A6 protein, stem xylem tissue from the transgenic *Populus* was ground into a fine powder in liquid nitrogen and then extracted in an equal volume of 2 × loading buffer [0.1 M Tris–HCl (pH 6.8), 4% Sodium Dodecyl Sulfate (SDS), 0.2% bromophenol blue, 20% glycerol]. After centrifugation at 12,000*g* for 10 min, the supernatant samples were separated by SDS-Polyacrylamide Gel Electrophoresis (PAGE), transferred onto a Polyvinylidene Fluoride Membrane (PVDF) membrane, and immunoblotted using the specific antibodies against PdCel9A6 (Yu et al. 2013). The protein levels were assessed using ImageJ software to examine the band intensities in western blot images.

Morphological analysis

Approximately 21 positive lines of *pCAMBIA2300:PdDUF579-9p-35Smini-PdCel9A6* (P_{D579}*-Cel*) transgenics and 17 positive lines of *pCAMBIA2300:PdWND1Bp-35Smini-PdCel9A6* transgenics (*Promoter(W1B)-Cel9A6-*) were identified, respectively. Two of them were selected based on a stable, similar level of expression and clonally propagated through micro-cutting for detailed characterization. The transgenics growing in a phyton were examined for phenotypic changes. The transgenic plants were grown in the field for two growing seasons and were harvested for pulping.

Mechanical strength analysis

The mechanical strength of the 12th–15th internodes of fresh stems was measured using a mechanical testing machine (HY-0580, Shanghai Hengyi Precision Instrument Co., Ltd), and the modulus of rupture (MOR) was calculated as described (Kern et al. 2005).

Microscopic analysis of wood tissues

The stem sample of the 12th–15th internodes was cut into a 5-mm segment and fixed in formalin-aceto-alcohol solution under vacuum, stored at 4 °C overnight, dehydrated in a graded ethanol series and embedded into paraffin. Samples were sectioned to a 10-μm thickness using a Leica RM2235 rotary microtome. Phloroglucinol-HCl staining was used for lignin detection as described (Gui et al. 2011). Toluidine blue staining was performed as described (Cao et al. 2020). The diameters of fiber cells and vessel cells were measured using ImageJ software. Cell wall thickness was observed using a transmission electron microscope as described (Xi et al. 2017). Stem samples were cut into 2-mm segments, fixed in 3% (v/v) paraformaldehyde and 0.5% (v/v) glutaraldehyde in PBS (0.1 M, pH 7.4), dehydrated in a graded ethanol series, embedded in Epon812 and sectioned. The samples were stained with 2% (w/v) uranyl acetate and lead citrate and observed under a transmission electron microscope (Hitachi H-7650). Secondary cell wall thickness was measured with ImageJ software (https://imagej.nih.gov/ij/download.html).

Fiber cell length measurement

Stem (the 15th internode) was debarked and cut into 2-cm lengths and disaggregated by submerging in a glacial acetic acid/30% hydrogen peroxide (v/v 1:1) solution at 60 °C overnight, stained with 1% (w/v) safranine for 10 min, and photographed under a light microscope (Olympus, BX53). Afterward, fiber length was measured according to the methods described by P.Zhang et al. (2012) using the Lorentzen & Wettre Fiber Tester (AB Lorentzen & Wettre, Kista, Sweden).

Cell wall composition analysis

Stem xylem tissue (16th–20th internodes) was collected and dried at 65 °C overnight. The dried tissue was ground to a fine powder and used to prepare alcohol-insoluble residues (AIR) (Song et al. 2014). For analysis of the sugar in hemicelluloses, AIR was treated with 2 M trifluoroacetic acid (TFA) at 121 °C for 90 min. The supernatant was evaporated and incubated in 20 mg mL^{-1} of fresh sodium borohydride solution at 40 °C for 90 min. The product was then neutralized with acetic acid and mixed with 1-methylimidazole and acetic anhydride for acetylation. After extraction with dichloromethane, the product was mixed with ethyl acetate for Gas Chromatography - Mass Spectrometry (6890 N GC system and 5975 Mass detector, Agilent Technologies, equipped with an SP-2380 capillary column, Supelco, Sigma-Aldrich) analysis. Meanwhile, standard sugars were used to calibrate the sugar content determined in samples. The insoluble precipitate from the AIR treated with TFA was collected for crystalline cellulose content determination. The Updegraff reagent (acetic acid:nitric acid:water, 8:1:2, v/v) was added to the precipitate and incubated at 100 °C for 30 min. After washing with H_2O and acetone, the precipitate was incubated with 72% sulfuric acid at room temperature for 1 h. The content of crystalline cellulose was determined by anthrone assay (Foster et al. 2010*b*). For lignin measurement, AIR was incubated with freshly prepared acetyl bromide (25% acetyl bromide in acetic acid) at 50 °C for 3 h. After cooling, the AIR was mixed with 2 M NaOH, 0.5 M fresh hydroxylamine hydrochloride and acetic acid. Lignin content was determined using a microplate reader (Varioskan Flash, Thermo) (Foster et al. 2010*a*).

RNA sequencing

Total RNA isolation was described as above for quantitative RT-PCR analysis. After the RNA quality was confirmed, 5 μg of the total RNA was used to construct a cDNA library using the TruSeq Stranded mRNA LT Sample Prep Kit (Illumina, RS-122-2101) and Agencourt AMPure XP (Beckman Coulter, A63881). The cDNA library was quality examined using the Agilent 2100 Bioanalyzer and then sequenced using the 150 bp paired-end sequencing strategy, which was performed on the Illumina HiSeq X10 platform. Raw data (raw reads) were processed using the NGS QC Toolkit (Patel and Jain 2012). Clean reads were mapped to the genome of *P. trichocarpa* (http://phytozome.jgi.doe.gov/) using the Hierarchical Indexing for Spliced Alignment of Transcripts 2 (HISAT 2) program with default parameters (Kim et al. 2015). Fragments per kilobase per million were calculated using Cufflinks (Roberts et al. 2011). To identify differentially expressed genes (DEGs) between different samples, the expression level of each transcript was calculated according to the transcripts per million reads method. Differential expression analysis was performed using the DESeq2/DEGseq/EdgeR with adjusted P value ≤ 0.05, DEGs with $|\log2FC| > 1$ and adjusted P value ≤ 0.05 (DESeq2 or EdgeR) were considered to be significantly different expressed genes. Kyoto Encyclopedia of Genes and Genomes (KEGG) pathway enrichment analysis of DEGs was performed using R based on the hypergeometric distribution (Kanehisa et al. 2008).

Paper property determination

Wood chips were produced from the trees grown in the field for two growing seasons. About 100 g of wood chips were utilized for pulping in a 1-L autoclave containing 1.32 mL of 0.1 M NaOH, 1.2 mL of 0.1 M Na_2S and 597.48 mL of H_2O according to the protocol used in the laboratory (Huang et al. 2014). After being soaked at 80 °C for 1 h, the wood chips were further heated to 170 °C for 2 h. Following the purification of the black liquor, the wood pulp underwent a drying process for 48 h. About 2 g of dry pulp were suspended in 5 L of water and processed to make paper using a circular paper-forming machine (Fuaibo Pulp and Paper Technology Development (Guangdong) Co., Ltd). The paper was desiccated in an atmosphere at 25 °C with 60% humidity for 48 h to equilibrate moisture content. In accordance with the TAPPI Method T404, T414 and T403 (Ma and Zhai 2013, Yoshihara and Yoshinobu 2014), the assessment of elongation, tensile strength and tear index was conducted utilizing a tensile tester (Guangzhou Biao Ji Packaging Equipment) and a tear resistance apparatus (PY-H610, Shenzhen Puyun Technology). Ten replicates of the paper samples were evaluated.

Result

Morphologies of the transgenics

In our previous studies, we have shown that the downregulation of *PtrCel9A6* expression under the control of the *Cauliflower Mosaic Virus* (*CaMV*) 35S promoter resulted in defects in xylem development and decreased cellulose content. Conversely, overexpression of *PtrCel9A6* under the control of the *CaMV* 35S promoter did not show any significant morphologic change (Yu et al. 2013). In this study, we explore the fiber cell-specific expression of the *PdCel9A6* in *P. deltoides* × *P. euramericana* cv. *Nanlin895*.

We constructed the expression vectors using the fiber cell-specific promoters *PdDUF579* and *PdWND1B* (Cao et al. 2020, Gui et al. 2020). The transgenic plants that harbored *DUF579-35Smini-PdCel9A6* were designated as P_{D579}-*Cel* and *WND1B-35Smini-PdCel9A6* as P_{W1B}-*Cel*, respectively.

Twenty-one independent P_{D579}-*Cel* transgenic lines were identified, and two representative transgenic lines (P_{D579}-*Cel-10* and P_{D579}-*Cel-50*) were clonally propagated for detailed characterization (Figure 1A and B). Simultaneously, 17 independent P_{W1B}-*Cel* transgenic lines were isolated. Two representative transgenic lines, namely P_{W1B}-*Cel-53* and P_{W1B}-*Cel-56*, were clonally propagated and used for detailed characterization (Figure 1A and B). In comparison with the wild type (WT), P_{D579}-*Cel* and P_{W1B}-*Cel* showed up-regulation of the *PdCel9A6* expression at both transcriptional and protein levels in developing xylem (Figure 1C and D). The height of P_{D579}-*Cel* and P_{W1B}-*Cel* plants was increased by 19.5% and 14.3%, respectively (Figure 1E). The internode length markedly increased in both P_{D579}-*Cel* and P_{W1B}-*Cel* plants (Figure 1F), whereas the stem diameter decreased by 17.1% in P_{D579}-*Cel* and 15.5% in P_{W1B}-*Cel* (Figure 1G). Meanwhile, measurement of the stem mechanical strength indicated that the MOR was decreased in P_{D579}-*Cel* and P_{W1B}-*Cel* transgenics (Figure 1H).

Stem anatomy of the transgenics

The modifications in the stem growth morphology of P_{D579}-*Cel* and P_{W1B}-*Cel* suggest possible changes in xylem development. During the stem secondary growth of the studied *Populus* species under our phytotron conditions, the vascular cambium ring, formed in the 5th to 6th internodes (Zhu et al. 2018, Xie et al. 2023), undergoes periclinal division to produce secondary xylem tissue organized in files. The formation of secondary cell walls in a file of cells typically completes at the 10th to 12th layers, where cell size and wall thickness are determined and can be observed at the 12th to 15th internodes (Xi et al. 2017, Xie et al. 2023). Subsequently, we performed an analysis of the growth of stem xylem at the 15th internodes. Both P_{D579}-*Cel* and P_{W1B}-*Cel* exhibited a significantly reduced development of xylem width (Figure 2A). Nevertheless, the quantity of cell layers in xylem tissue remained unchanged (Figure 2B). Measurement of cell size in the xylem indicated a reduction in fiber diameter, but the vessel diameter exhibited no significant differences (Figure 2C–E). The findings demonstrate that the overexpression of *PdCel9A6* influenced fiber cell dimensions.

Characteristics of fiber cells in the transgenics

To further study fiber cell characteristics in the transgenics, we performed longitudinal dissection of stems to assess xylem fiber cell length. Microscopic examination indicated that the fiber cell length in P_{D579}-*Cel* and P_{W1B}-*Cel* was longer (Figure 3A) than that in WT. To precisely determine their length, we isolated the fibers in the xylem and measured their lengths. The results demonstrated that the fiber cell length in P_{D579}-*Cel* and P_{W1B}-*Cel* increased by 24.1% and 22.5%, respectively, compared with the WT (Figure 3B). In addition, the P_{D579}-*Cel* and P_{W1B}-*Cel* transgenics exhibited reduced thickness in fiber cell walls (Figure 3C and D). Examination of the cell wall composition of wood tissue indicated a reduction in lignin content alongside an elevation in cellulose content, while the monosaccharide composition of glucose, fucose and arabinose showed an increase in both P_{D579}-*Cel* and P_{W1B}-*Cel* but the composition of rhamnose, xylose and galactose exhibited a decrease (Figure 3E–G). The findings indicate that the *PdCel9A6* overexpression modified xylem fiber length and cell wall biosynthesis, leading to changes in cellulose and lignin deposition.

Transcriptional profile in the developing xylem of transgenics was changed

As the fiber cell characteristics in transgenics were modified, we performed transcriptomic analysis to find how the transcription activities were modulated by *PdCel9A6* overexpression. The developing xylem tissue was collected for transcriptome sequencing (see Figure S1 available as Supplementary Data at *Tree Physiology* Online). It was detected that there are 4242 genes that were differentially expressed (fold change >2) between P_{D579}-*Cel* and WT, including 1431 genes up-regulated and 2811 genes down-regulated (Figure 4A and Table S2 available as Supplementary Data at *Tree Physiology* Online). These DEGs are enriched in multiple aspects of biological processes, cellular components and molecular functions (Figure 4B). The genes that were involved in plant hormone signal transduction, sugar metabolism and other processes were upregulated (Figure 4C). The down-regulated genes were mainly involved in plant–pathogen interaction, phenylpropanoid biosynthesis and other pathways (Figure 4D). Genes that are related to gibberellin and BR1 signaling (Figure 5A and B and Table S3 available as Supplementary Data at *Tree Physiology* Online) showed an increased expression, which suggests that gibberellins and BR may affect fiber cell elongation. On the other hand, the expression of the genes involved in lignin biosynthesis, such as *CCR* and *COMT* was decreased (Figure 5B) in the transgenics, which was in line with the decreased lignin content.

The characteristics of the paper processed from the transgenics

The transgenics showed an increase of fiber length during early growth in the greenhouse. Then we examined the P_{D579}-*Cel* transgenic growth in the field (Figure 6A and B). After a period of two growth seasons, the transgenics displayed higher growth and a smaller size of diameter at breast height (DBH) (Figure 6C and D). The longer fiber characteristic of the transgenics was sustained in field growth (Figure 6E and F).

Then we collected the transgenic wood material to make pulp and paper (Figure 6G and H). Analysis of the mechanical properties of the paper showed that the paper processed from the wood material of P_{579}-*Cel* displayed stronger stretch at break and tensile strength (Figure 6I). The transgenic *Populus* showed higher pulping yield and improvement of paper mechanical properties when applied to making paper (Figure 6J). This could be attributed to the longer fibers and the changes in cell wall compositions in the transgenic wood.

Discussion

The growth and development of vascular plants result from cellular division and differentiation within diverse tissues. Xylem fibers are a primary cell type formed during secondary growth of stems by vascular cambium division, providing mechanical support in angiosperm trees.

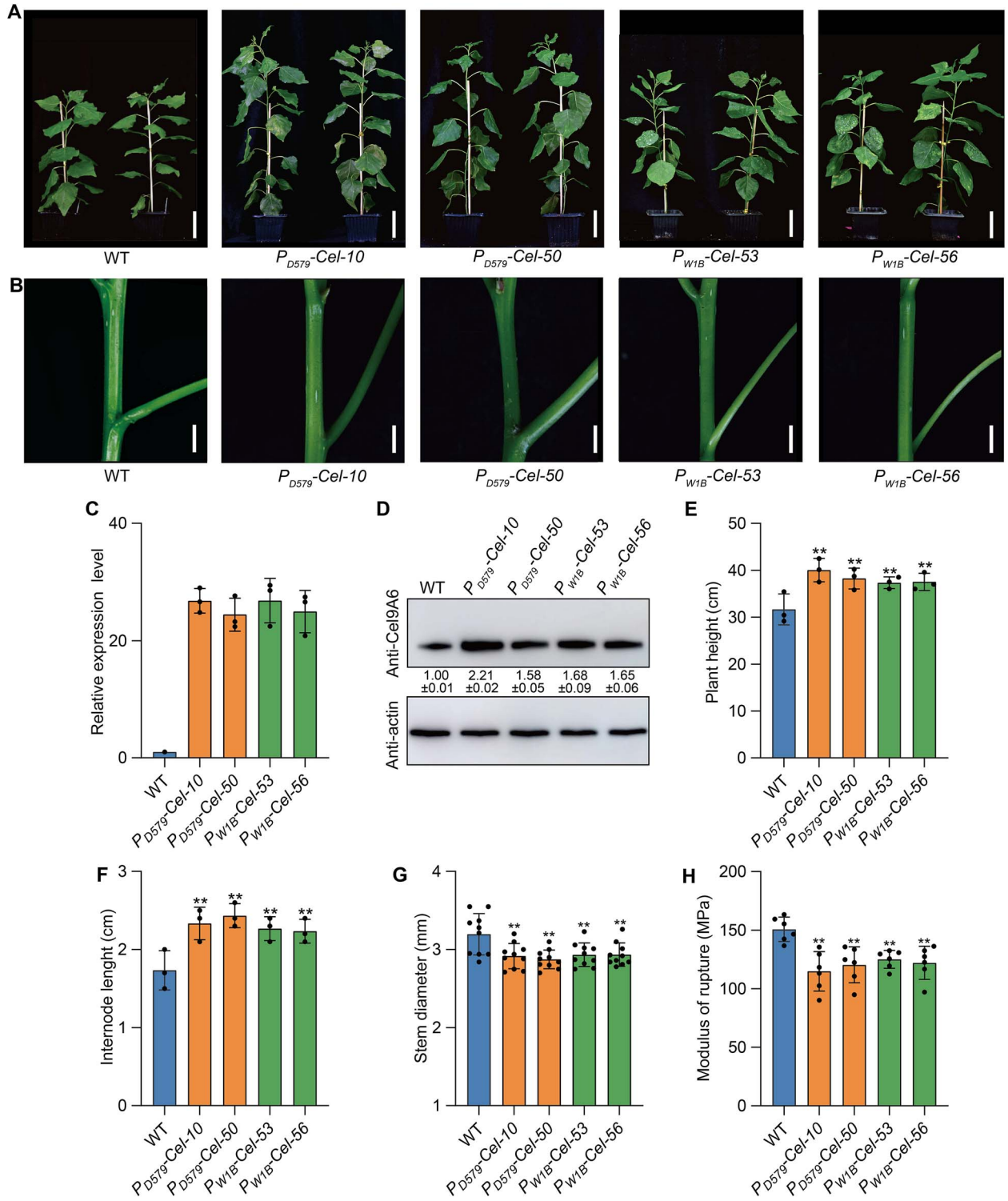

Figure 1. The growth morphologies of the fiber cell-specific upregulation of *PdCel9A6* in *Populus*. (A, B) Transgenics of P_{D579}-*Cel* and P_{W1B}-*Cel* at 2 months old. Scale bar, 6 cm in (A) and 0.6 cm in (B). (C) The *PdCel9A6* expression in the transgenic xylem tissue compared with that in WT (the expression in WT is set to 1). The *ACTIN* gene (*Potri.001G309500*) is used as a reference for expression normalization. (D) Western blot analysis of the *PdCel9A6* protein in the developing xylem of the transgenics. (E) Plant height, (F) Internode length (the 15th internode) and (G) stem diameter. (H) Stem mechanical strength. The means ± SD is calculated based on data obtained from three clonally propagated plants. Asterisks (**) indicate significant differences, $P < 0.01$ (Student's t-test).

Fiber cells in hard wood serve as a primary resource for paper production, and their characteristics substantially affect the attributes of the resultant paper product (Pulkkinen et al. 2006). Longer fibers enhance tensile and burst strength through increased overlapping and bonding sites, forming a strong structure in paper, reduce pull-out probability by bridging gaps, making them appropriate for packaging materials like grocery bags, establish effective flexibil-

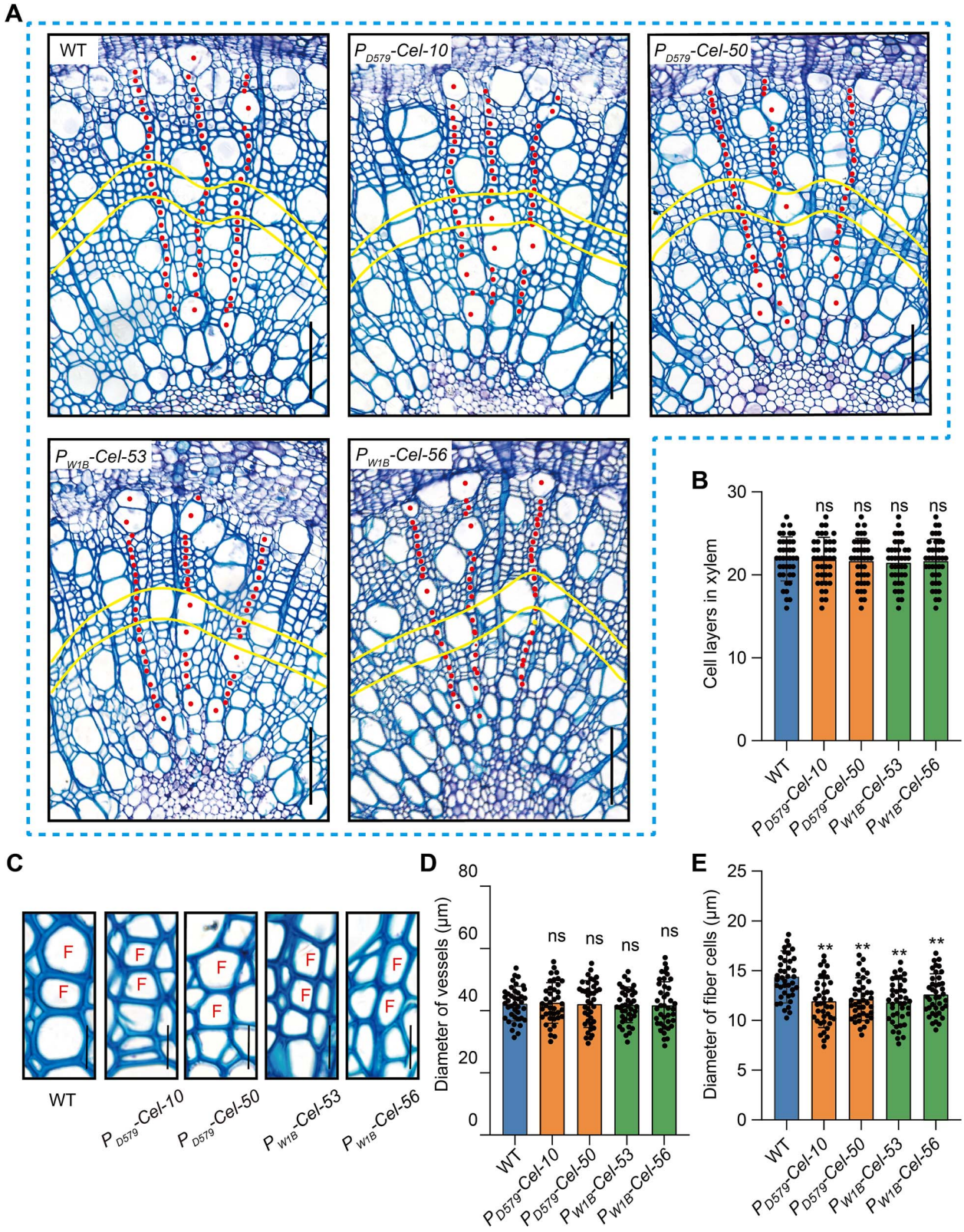

Figure 2. Stem cross-anatomy of the P_{D579}-*Cel* and P_{W1B}-*Cel*. (A) Stem cross-sections (the 15th internode) of P_{D579}-*Cel* and P_{W1B}-*Cel* stained with toluidine blue. The dots indicate xylem cells arranged in a file, and 40 files were examined in each transgenic line. The curve marks an area of the xylem cells at the 12th–15th layers in a file that was examined for cell morphology. Scale bar, 100 μm. (B) Cell layers in a file of xylem cells. (C) Cross-view of xylem fibers. F, fiber cell. Scale bar, 16 μm. (D) Diameter of vessels. (E) Diameter of fiber cells. The results are mean ± SD based on the determination of 40 cells. Asterisks (**) indicate significant differences, $P < 0.01$ (Student's *t*-test). 'ns' indicates no significant difference.

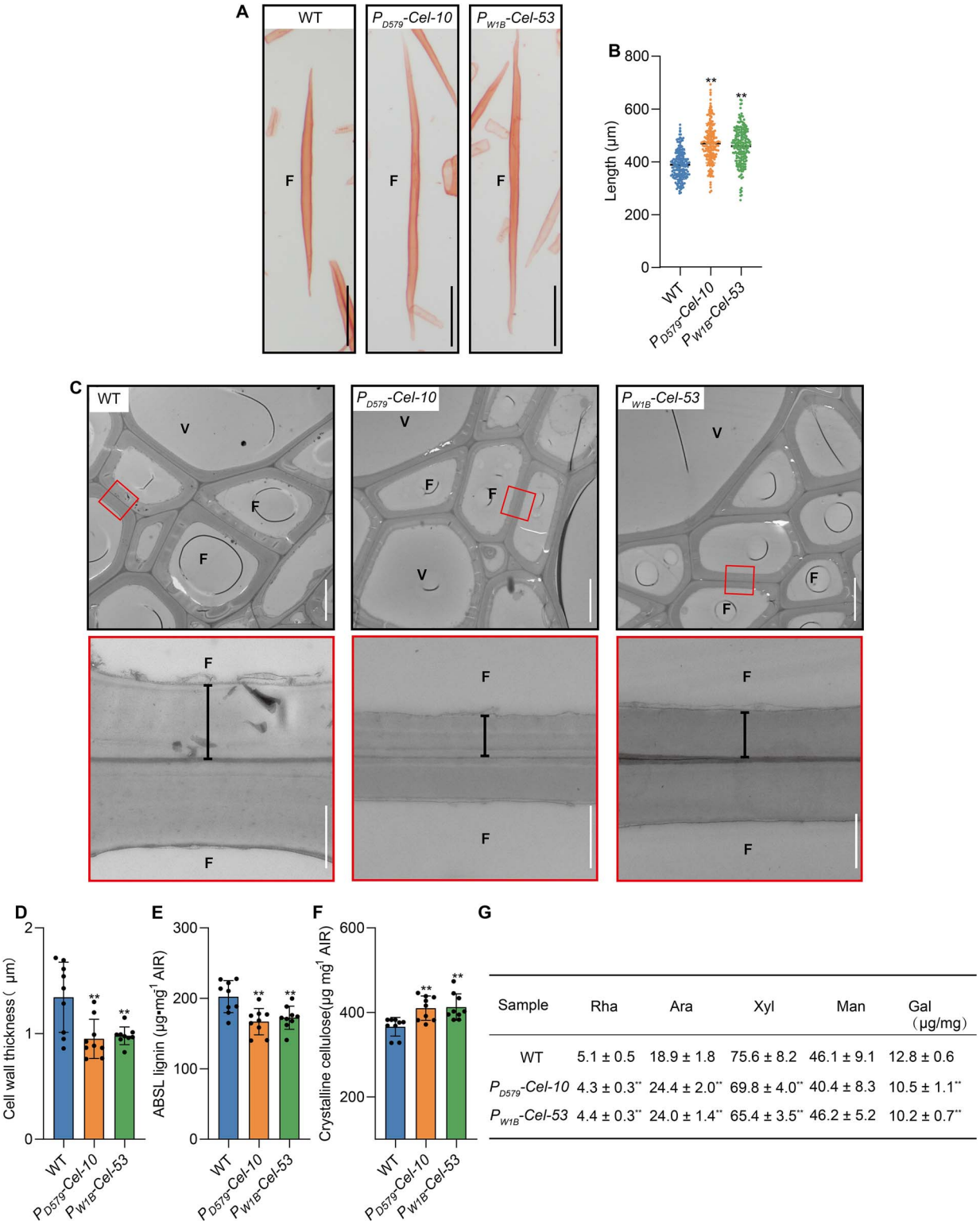

Sample	Rha	Ara	Xyl	Man	Gal (μg/mg)
WT	5.1 ± 0.5	18.9 ± 1.8	75.6 ± 8.2	46.1 ± 9.1	12.8 ± 0.6
P_{D579}-Cel-10	4.3 ± 0.3**	24.4 ± 2.0**	69.8 ± 4.0**	40.4 ± 8.3	10.5 ± 1.1**
P_{W1B}-Cel-53	4.4 ± 0.3**	24.0 ± 1.4**	65.4 ± 3.5**	46.2 ± 5.2	10.2 ± 0.7**

Figure 3. The properties of fiber cells. The 15th internode of fiber cell length, cell wall thickness and cell wall composition were measured in the 15th internode of P_{D579}-*Cel-10* and P_{W1B}-*Cel-53*. (A) Dissociated fibers were observed under an optical microscope. Scale bar, 100 μm. F, fiber cell. (B) The length of the dissociated fibers. (C) Transmission electron micrographs of fiber cell walls in P_{D579}-*Cel* and P_{W1B}-*Cel*. F, fiber cell. V, vessel cell. Scale bar, 6 μm. The magnification of the fiber cell wall is marked in rectangles and the lines indicate the thickness of the cell wall. Scale bar, 1.2 μm. (D) Cell wall thickness; (E) lignin content; (F) cellulose content and (G) hemicellulose monosaccharide content in P_{D579}-*Cel* and P_{W1B}-*Cel*. Cell wall thickness: means ± SD of nine fiber cells from each of three clonally propagated plants. Lignin and cellulose content: means ± SD of tree samples from each of three clonally propagated plants. Hemicellulose monosaccharide content: means ± SD of three samples from each of three clonally propagated plants. Asterisks (**) indicate significant differences, $P < 0.01$ (Student's *t*-test). 'ns' indicates no significant difference.

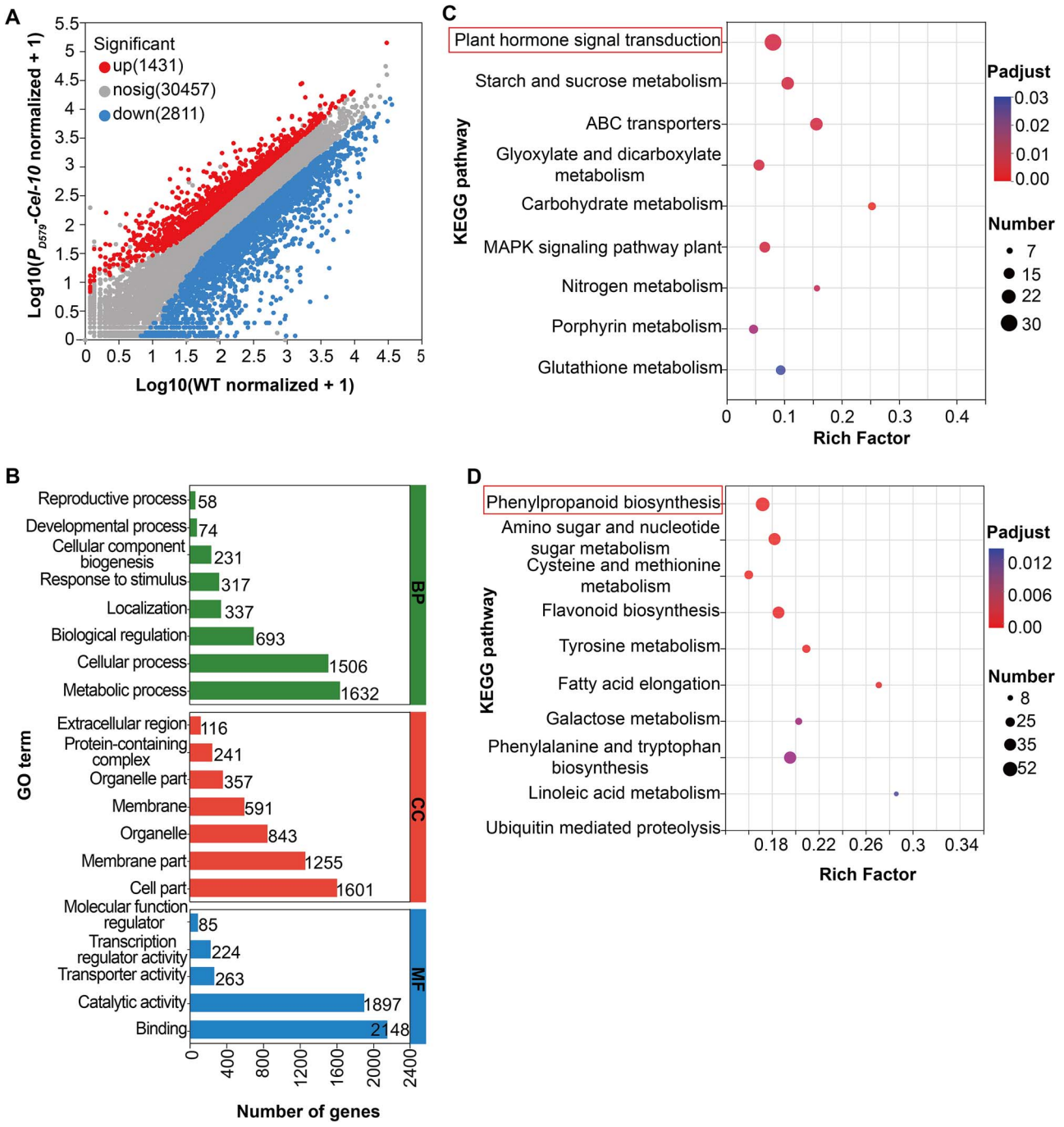

Figure 4. RNA sequencing of the stem xylem tissue in *P_{D579}-Cel-10* and WT. (A) Volcano map of DEGs between *P_{D579}-Cel-10* and WT. Each dot represents a specific gene, with those in the upper left quadrant indicating significant up-regulation, those in the lower right quadrant indicating significant down-regulation, and those along the diagonal representing non-significant differential expression. (B) GO annotation of the DEGs between *P_{D579}-Cel-10* and WT. (C) KEGG enrichment of the *P_{D579}-Cel-10* up-regulated genes. (D) KEGG enrichment of *P_{D579}-Cel-10* down-regulated genes. P-adjust and rich factor are indicated.

ity and connectivity, thereby enhancing paper durability (Gharehkhani et al. 2015, Larsson et al. 2018). In addition to fiber length, other characters such as cell wall composition and lignin content are also crucial factors influencing pulping efficiency (Baucher et al. 2003). The modern pulping industry has paid attention to precise regulation of fiber properties through bio-based nanotechnology, post-pretreatment of Kraft and sulfite pulps and bioengineering of wood cell walls to improve pulping efficiency (Mboowa 2024). The presence of lignin in wood makes it recalcitrant to pulping, requiring harsh chemical delignification processes for the production of high-quality paper. Thus, recent research efforts have been dedicated to engineering lignin amount and composition to overcome these problems (De Meester et al. 2022, Zhu and Li 2024). In the last two decades, many studies have demonstrated that genetic engineering can generate trees with low lignin content and readily degradable lignin; however, this technology has not been extensively employed to engineer trees suitable for pulping and papermaking because the lignin modifications may impact the growth of trees in the

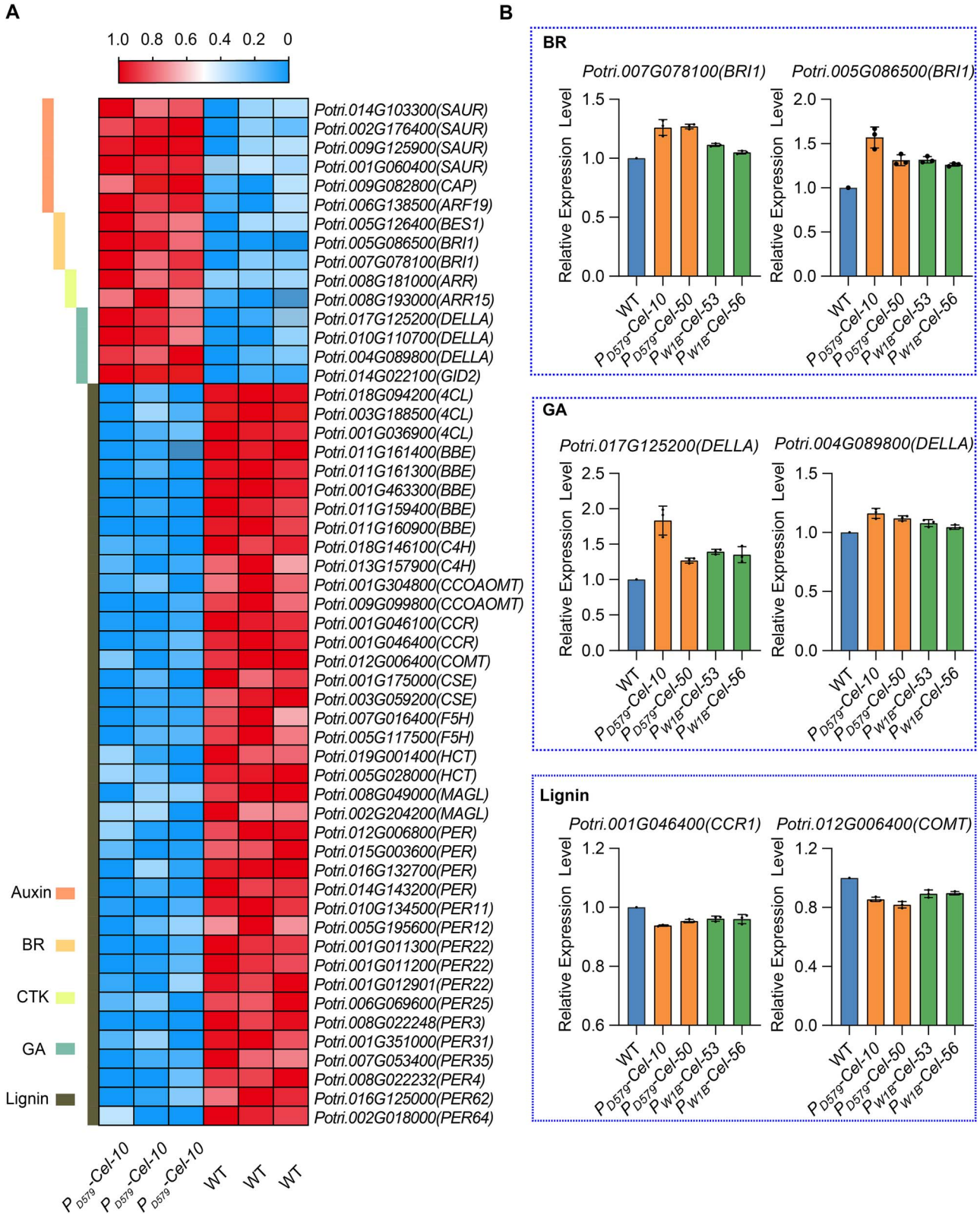

Figure 5. Differentially expressed genes (DEGs) in P_{D579}-*Cel-10* were enriched in hormone signaling and lignin biosynthesis. (A) Heat maps of the genes associated with hormone signals and lignin biosynthesis. (B) RT-PCR confirmation of the differential expression of key genes involved in brassinosteroids (*BRI1*), gibberellins signaling (*DELLA*) and lignin biosynthesis (*COMT*, *F5H* and *CCR*). Data are means ± SD of three independent plants.

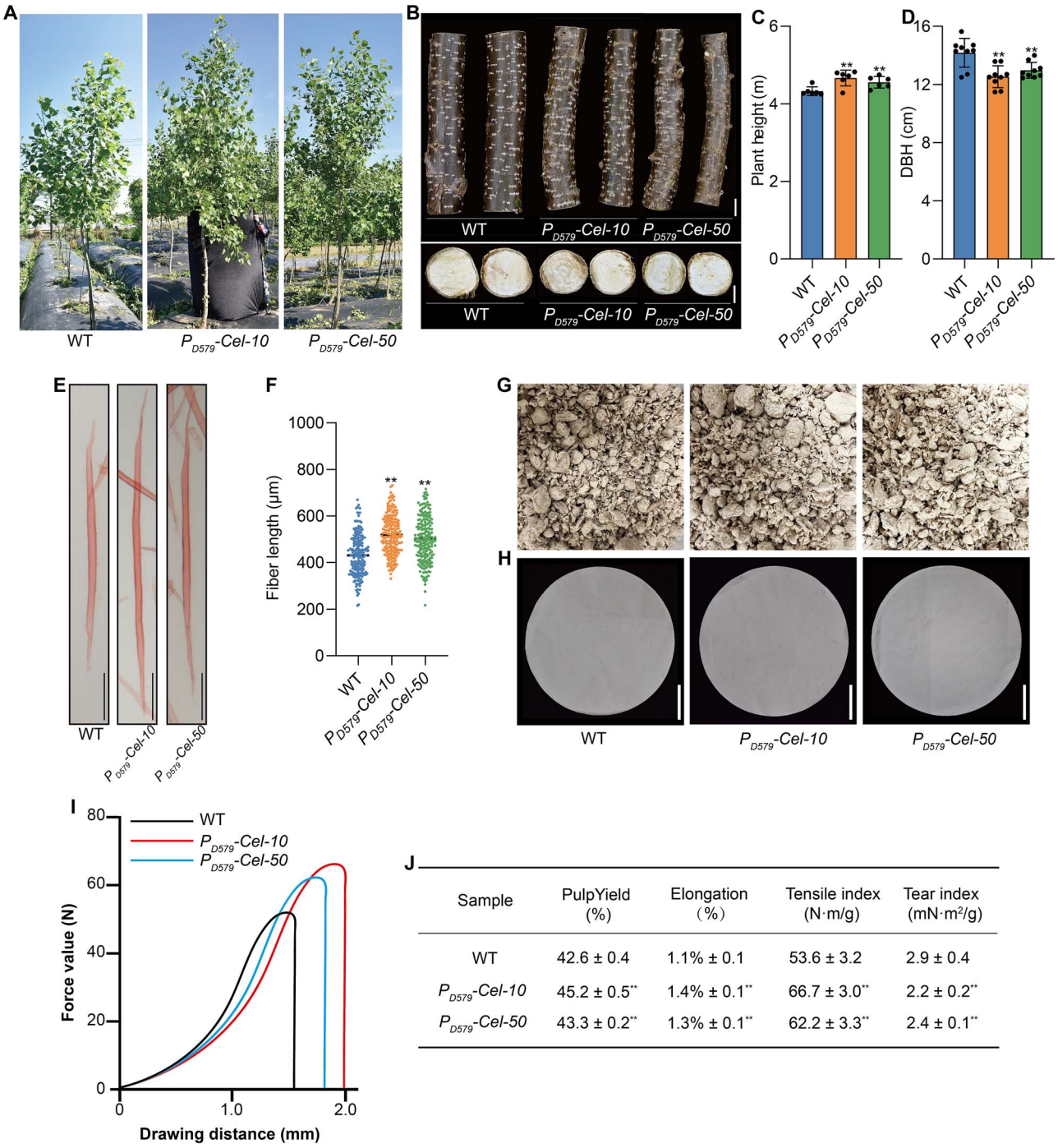

J

Sample	PulpYield (%)	Elongation (%)	Tensile index (N·m/g)	Tear index (mN·m²/g)
WT	42.6 ± 0.4	1.1% ± 0.1	53.6 ± 3.2	2.9 ± 0.4
P_{D579}-Cel-10	45.2 ± 0.5**	1.4% ± 0.1**	66.7 ± 3.0**	2.2 ± 0.2**
P_{D579}-Cel-50	43.3 ± 0.2**	1.3% ± 0.1**	62.2 ± 3.3**	2.4 ± 0.1**

Figure 6. Field growth of the transgenic trees and papermaking test. (A) The P_{D579}-*Cel* transgenic trees were grown in the field for a period of two growing seasons. (B) Wood stem harvested from field-grown trees. Bar, 5 cm. (C) Tree height and (D) DBH. (E) Fibers dissociated from field-grown trees. Scale bar, 50 μm. (F) Fiber length from field-grown trees. Data were collected from three biological replicates, and more than 200 fibers were measured. (G) Wood chips were harvested for pulping. (H) Processed paper from the wood chips. Scale bar, 4 cm. (I) The breaking force and tensile length of the paper. (J) Properties of the paper processed from the wood chip. Data are means ± SD of 10 pieces of paper. Asterisks (**) indicate significant differences, $P < 0.01$ (Student's *t*-test).

field (De Meester et al. 2022, Zhu and Li 2024). Recent studies demonstrated that fiber cell-specific modification of lignin biosynthesis reduces lignin content while preserving healthy field growth (Cao et al. 2020, Gui et al. 2020). The development of new trees with optimized growth and lignin content will significantly benefit the pulp and paper industry.

During wood development, fiber cells undergo significant elongation, regulating their length. A variety of proteins and enzymes facilitate cell wall relaxation to permit cell expansion and elongation (Luo et al. 2021, Zhu and Li 2021, Luo and Li 2022). Expansins are proteins that facilitate the loosening of the cell wall, enabling its extension (Yu et al. 2013). Xyloglucan endo-transglycosylases modify the xyloglucan-cellulose structure of plant cell walls, hence regulating their expansion (Gray-Mitsumune et al. 2004, Hao et al. 2024). EGase catalyzes the hydrolysis of 1,4-β-

D-glucan chain molecules, hence promoting the relaxation of the cell wall and enabling cellular expansion and elongation (Urbanowicz et al. 2007*b*, Yu et al. 2013). In previous studies, we employed the *CaMV 35S* promoter to upregulate the expression of *PtrCel9A6* in *Arabidopsis* and *Populus* (Yu et al. 2013). The transgenic Arabidopsis exhibited a notable increase in cell size in both leaf and stem, with modifications in cell wall thickness observed in certain tissues (Yu et al. 2013). Cell type-specific modifications of the cell wall have been successfully achieved in *Arabidopsis* and *Populus* (Cao et al. 2020, Gui et al. 2020, Rich-Griffin et al. 2020). Modification of lignin biosynthesis specific to fiber cells during wood formation led to a reduction in lignin content, while allowing for normal growth both in greenhouse and field conditions (Cao et al. 2020, Gui et al. 2020), thereby demonstrating the significant potential of this strategy for engineering wood cell wall characteristics without hindering growth. *Populus DUF579* and *WND1B* are preferentially expressed in fiber cells to contribute to their cell wall formation (Song et al. 2014, Zhao et al. 2014, Song et al. 2016). This study employed these fiber-cell-specific gene promoters to regulate the expression of *PdCel9A6*. Both transgenic *Populus* exhibited elongated internode lengths in the stem, which comprised longer fiber cells (Figures 1B, F and 3A, B). This may be due to the overexpression of *PdCel9A6* in fiber cells that leads to cell wall loosening and subsequent fiber cell elongation. Meanwhile, it was observed that the thickness of fiber cell walls and the composition of wood, including lignin and cellulose content, were modified (Figure 3D–F). Cell elongation and wall thickening are two processes coordinately regulated; studies suggest that oligosaccharides may act as signals to regulate the coordination (Zhao et al. 2013, Zhang et al. 2024). The overexpression of *PdCel9A6* led to cell elongation while simultaneously influencing secondary cell wall deposition. In line with this, transcriptional analysis indicates that the expression of *PdCel9A6* changed the transcriptional activities in the regulation of cell elongation as well as cell wall thickening (Figures 4A–C and 5A, B). The expression of gibberellin and BR1 signaling pathway genes and secondary cell wall formation genes is modified, although the specific mechanisms underlying these transcriptional modifications warrant more investigation. This observation provides insight into the transcriptional regulation between fiber elongation and cell wall thickening.

Overexpression of the *PdCel9A6* gene in xylem fiber cells increased height growth and wood fiber cell length in *Populus*. These traits of the transgenics remained stable after two growing seasons in the field (Figure 6A–F). When the transgenic trees grown in the field were used for pulping and papermaking, the mechanical properties of the resultant paper, including breaking strength, tensile strength and elongation, were increased (Figure 6I and J). This should be attributed to the changes in the fiber cell properties of the transgenic *Populus*. Previous studies showed modification of lignin biosynthesis in fiber cells (Cao et al. 2020, Gui et al. 2020); the present study demonstrates that the length of wood fiber cells can also be manipulated by genetic engineering. The engineering of the properties of wood fiber cells would enable the development of new strategies to create trees tailored for specific wood material applications.

In conclusion, the targeted overexpression of *PdCel9A6* in fiber cells resulted in increased fiber length in *Populus*. After growing in the field for two growing seasons, this genetically modified tree showed healthy growth and, when applied to papermaking, yielded important improvements in the paper's mechanical properties. Consequently, extensive field-testing and comprehensive assessments should be undertaken to propel this technology toward industrial implementation.

Acknowledgments

We thank Xiaoyan Gao, Jiqin Li and Zhiping Zhang for assistance with TEM. We appreciate assistance from Dr Wenli Hu for GC-MS analysis. We would also like to express our gratitude to Wu Wenjuan from Nanjing Forestry University for assistance in pulping experiment.

Supplementary data

Supplementary data for this article are available at *Tree Physiology* Online.

Author contributions

J.L., M.L. and L.L. designed the research. J.L., X.G. and X.L. performed biological experiments. J.S. conducted genetic transformation. J.L. performed pulping and papermaking experiments. J.L., X.G., Y.J., M.L. and L.L. analyzed the data. J.L., M.L. and L.L. wrote the paper. All authors read and approved the article.

Conflict of interest

None declared.

Funding

This work was supported by the National Key Research and Development Program (2021YFD2200204), the Strategic Priority Research Program of the Chinese Academy of Sciences (XDB0630203) and the National Natural Science Foundation of China (32130072) to L.L.

Data availability

The data that support the findings of this study are available in supplementary materials. Specific data that were not included in the supplementary materials are available on request from the corresponding author, L.L.

References

Aggarwal D, Kumar A, Reddy MS (2015) Genetic transformation of endo-1,4-β-glucanase (Korrigan) for cellulose enhancement in *Eucalyptus tereticornis*. Plant Cell Tissue Organ Cult 122:363–371. https://doi.org/10.1007/s11240-015-0774-7.

Baucher M, Claire H, Michel P-C, Oerjan W (2003) Lignin: genetic engineering and impact on pulping. Crit Rev Biochem Mol Biol 38: 305–350. https://doi.org/10.1080/10409230391036757.

Cao S, Huang C, Luo L, Zheng S, Zhong Y, Sun J, Gui J, Li L (2020) Cell-specific suppression of 4-Coumarate-CoA ligase gene reveals differential effect of lignin on cell physiological function in Populus. Front Plant Sci 11:589729. https://doi.org/10.3389/fpls.2020.589729.

De Meester B, Vanholme R, Mota T, Boerjan W (2022) Lignin engineering in forest trees: from gene discovery to field trials. Plant Commun 3:100465. https://doi.org/10.1016/j.xplc.2022.100465.

Du Q, Wang L, Yang X, Gong C, Zhang D (2015) Populus endo-β-1, 4-glucanases gene family: genomic organization, phylogenetic analysis, expression profiles and association mapping. Planta 241: 1417–1434. https://doi.org/10.1007/s00425-015-2271-y.

Eriksson ME, Israelsson M, Olsson O, Moritz T (2000) Increased gibberellin biosynthesis in transgenic trees promotes growth, biomass production and xylem fiber length. Nat Biotechnol 18:784–788. https://doi.org/10.1038/77355.

Foster CE, Martin TM, Pauly M (2010*a*) Comprehensive compositional analysis of plant cell walls (lignocellulosic biomass) part I: lignin. J Vis Exp **37**:1745. https://doi.org/10.3791/1745.

Foster CE, Martin TM, Pauly M (2010*b*) Comprehensive compositional analysis of plant cell walls (lignocellulosic biomass) part II: carbohydrates. J Vis Exp **37**:1837. https://doi.org/10.3791/1837.

Gharehkhani S, Sadeghinezhad E, Kazi SN, Yarmand H, Badarudin A, Safaei MR, Zubir MN (2015) Basic effects of pulp refining on fiber properties—a review. Carbohydr Polym 115:785–803. https://doi.org/10.1016/j.carbpol.2014.08.047.

Gray-Mitsumune M, Mellerowicz EJ, Abe H et al. (2004) Expansins abundant in secondary xylem belong to subgroup a of the alpha-expansin gene family. Plant Physiol 135:1552–1564. https://doi.org/10.1104/pp.104.039321.

Gui J, Shen J, Li L (2011) Functional characterization of evolutionarily divergent 4-coumarate:coenzyme a ligases in rice. Plant Physiol 157: 574–586. https://doi.org/10.1104/pp.111.178301.

Gui J, Lam PY, Tobimatsu Y, Sun J, Huang C, Cao S, Zhong Y, Umezawa T, Li L (2020) Fibre-specific regulation of lignin biosynthesis improves biomass quality in Populus. New Phytol 226: 1074–1087. https://doi.org/10.1111/nph.16411.

Guo X, Li J, Li M, Zhou B, Zheng S, Li L (2024) A molecular module connects abscisic acid with auxin signals to facilitate seasonal wood formation in Populus. Plant Cell Environ 47:4323–4336. https://doi.org/10.1111/pce.15027.

Hao Y, Chu L, He X, Zhao S, Tang F (2024) PagEXPA1 combines with PagCDKB2;1 to regulate plant growth and the elongation of fibers in *Populus alba* x *Populus glandulosa*. Int J Biol Macromol 268:131559. https://doi.org/10.1016/j.ijbiomac.2024.131559.

Huang C, Chu Q, Xie Y, Li X, Jin Y, Min D, Yong Q (2014) Effect of Kraft pulping pretreatment on the chemical composition, enzymatic digestibility, and sugar release of moso bamboo residues. BioResources 10:240–255. https://doi.org/10.15376/biores.10.1.240-255.

Junko T, Rudsander UJ, Mattias H et al. (2009) KORRIGAN1 and its aspen homolog PttCel9A1 decrease cellulose crystallinity in Arabidopsis stems. Plant Cell Physiol 50:1099–1115. https://doi.org/10.1093/pcp/pcp062.

Kanehisa M, Araki M, Goto S et al. (2008) KEGG for linking genomes to life and the environment. Nucleic Acids Res 36:D480–D484. https://doi.org/10.1093/nar/gkm882.

Kern KA, Ewers FW, Telewski FW, Koehler L (2005) Mechanical perturbation affects conductivity, mechanical properties and aboveground biomass of hybrid poplars. Tree Physiol 25:1243–1251. https://doi.org/10.1093/treephys/25.10.1243.

Kim D, Langmead B, Salzberg SL (2015) HISAT: a fast spliced aligner with low memory requirements. Nat Methods 12:357–360. https://doi.org/10.1038/nmeth.3317.

Larsson PT, Lindström T, Carlsson LA, Fellers C (2018) Fiber length and bonding effects on tensile strength and toughness of Kraft paper. J Mater Sci 53:3006–3015. https://doi.org/10.1007/s10853-017-1683-4.

Li L, Zhou Y, Cheng X, Sun J, Marita JM, Ralph J, Chiang VL (2003) Combinatorial modification of multiple lignin traits in trees through multigene cotransformation. Proc Natl Acad Sci U S A 100: 4939–4939, 4944. https://doi.org/10.1073/pnas.0831166100.

Li L, Cheng X, Lu S, Nakatsubo T, Umezawa T, Chiang VL (2005) Clarification of cinnamoyl co-enzyme a reductase catalysis in monolignol biosynthesis of aspen. Plant Cell Physiol 46:1073–1082. https://doi.org/10.1093/pcp/pci120.

Li W, Lin Y-CJ, Chen Y-L et al. (2024) Woody plant cell walls: fundamentals and utilization. Mol Plant 17:112–140. https://doi.org/10.1016/j.molp.2023.12.008.

Linton SM (2020) The structure and function of cellulase (endo-β-1, 4-glucanase) and hemicellulase (β-1, 3-glucanase and endo-β-1, 4-mannase) enzymes in invertebrates that consume materials ranging from microbes, algae to leaf litter. Comp Biochem Physiol Part B Biochem Mol Biol 240:110354. https://doi.org/10.1016/j.cbpb.2019.110354.

Liu S, Fu X, Wang Y et al. (2025) The auxin–PLETHORA 5 module regulates wood fibre development in *Populus tomentosa*. Nature Plants 11:580–594. https://doi.org/10.1038/s41477-025-01931-z.

Luo L, Li L (2022) Molecular understanding of wood formation in trees. Forest Res 2:0. https://doi.org/10.48130/FR-2022-0005.

Luo L, Zhu Y, Gui J, Yin T, Luo W, Liu J, Li L (2021) A comparative analysis of transcription networks active in juvenile and mature wood in Populus. Front Plant Sci 12:675075. https://doi.org/10.3389/fpls.2021.675075.

Ma P, Zhai H (2013) Selective TEMPO-mediated oxidation of thermomechanical pulp. BioResources 8:4396–4405. https://doi.org/10.15376/biores.8.3.4396-4405.

Maloney VJ, Samuels AL, Mansfield SD (2012) The endo-1,4-β-glucanase Korrigan exhibits functional conservation between gymnosperms and angiosperms and is required for proper cell wall formation in gymnosperms. New Phytol 193:1076–1087. https://doi.org/10.1111/j.1469-8137.2011.03998.x.

Mboowa D (2024) A review of the traditional pulping methods and the recent improvements in the pulping processes. Biomass Convers Biorefin 14:1–12. https://doi.org/10.1007/s13399-020-01243-6.

Noh SA, Choi YI, Cho JS, Lee H (2015) The poplar basic helix-loop-helix transcription factor BEE3—like gene affects biomass production by enhancing proliferation of xylem cells in poplar. Biochem Biophys Res Commun 462:64–70. https://doi.org/10.1016/j.bbrc.2015.04.109.

Ohmiya N, Nakai T, Park YW, Aoyama T, Oka A, Sakai F, Hayashi T (2003) The role of PopCel1 and PopCel2 in poplar leaf growth and cellulose biosynthesis. Plant J 33:1087–1097. https://doi.org/10.1046/j.1365-313X.2003.01695.x.

Park YW, Tominaga R, Sugiyama J, Furuta Y, Tanimoto E, Samejima M, Sakai F, Hayashi T (2003) Enhancement of growth by expression of poplar cellulase in *Arabidopsis thaliana*. Plant J 33:1099–1106. https://doi.org/10.1046/j.1365-313X.2003.01696.x.

Patel RK, Jain M (2012) NGS QC toolkit: a toolkit for quality control of next generation sequencing data. PLoS One 7:e30619. https://doi.org/10.1371/journal.pone.0030619.

Pulkkinen I, Ala-Kaila K, Aittamaa J (2006) Characterization of wood fibers using fiber property distributions. Chem Eng Process Process Intensif 45:546–554. https://doi.org/10.1016/j.cep.2005.12.003.

Rich-Griffin C, Eichmann R, Reitz MU et al. (2020) Regulation of cell type-specific immunity networks in Arabidopsis roots. Plant Cell 32: 2742–2762. https://doi.org/10.1105/tpc.20.00154.

Roberts A, Trapnell C, Donaghey J, Rinn JL, Pachter L (2011) Improving RNA-Seq expression estimates by correcting for fragment bias. Genome Biol 12:R22. https://doi.org/10.1186/gb-2011-12-3-r22.

Song D, Sun J, Li L (2014) Diverse roles of PtrDUF579 proteins in *Populus* and PtrDUF579-1 function in vascular cambium proliferation during secondary growth. Plant Mol Biol 85:601–612. https://doi.org/10.1007/s11103-014-0206-9.

Song D, Gui J, Liu C, Sun J, Li L (2016) Suppression of PtrDUF579-3 expression causes structural changes of the glucuronoxylan in Populus. Front Plant Sci 7. 493-505. https://doi.org/10.3389/fpls.2016.00493.

Urbanowicz BR, Bennett AB, Del Campillo E et al. (2007*a*) Structural organization and a standardized nomenclature for plant endo-1,4-beta-glucanases (cellulases) of glycosyl hydrolase family 9. Plant Physiol 144:1693–1696. https://doi.org/10.1104/pp.107.102574.

Urbanowicz BR, Catala C, Irwin D, Wilson DB, Ripoll DR, Rose JKC (2007*b*) A tomato endo-beta-1,4-glucanase, SlCel9C1, represents a distinct subclass with a new family of carbohydrate binding modules (CBM49). J Biol Chem 282:12066–12074. https://doi.org/10.1074/jbc.M607925200.

Xi W, Song D, Sun J, Shen J, Li L (2017) Formation of wood secondary cell wall may involve two type cellulose synthase complexes in *Populus*. Plant Mol Biol 93:419–429. https://doi.org/10.1007/s11103-016-0570-8.

Xie Z, Gui J, Zhong Y, Li B, Sun J, Shen J, Li L (2023) Screening genome-editing knockouts reveals the receptor-like kinase ASX role in regulations of secondary xylem development in *Populus*. New Phytol 238:1972–1985. https://doi.org/10.1111/nph.18881.

Yoshihara H, Yoshinobu M (2014) Effects of specimen configuration and measurement method of strain on the characterization of tensile properties of paper. J Wood Sci 60:287–293. https://doi.org/10.1007/s10086-014-1398-y.

Yu L, Sun J, Li L (2013) PtrCel9A6, an endo-1,4-β-glucanase, is required for cell wall formation during xylem differentiation in *Populus*. Mol Plant 6:1904–1917. https://doi.org/10.1093/mp/sst104.

Yu L, Chen H, Sun J, Li L (2014) PtrKOR1 is required for secondary cell wall cellulose biosynthesis in *Populus*. Tree Physiol 34:1289–1300. https://doi.org/10.1093/treephys/tpu020.

Yu L, Li Q, Zhu Y, Afzal MS, Li L (2018) An auxin-induced β-type endo-1, 4-β-glucanase in poplar is involved in cell expansion and lateral root formation. Planta 247:1149–1161. https://doi.org/10.1007/s00425-018-2851-8.

Zhang JW, Xu L, Wu YR, Chen XA, Liu Y, Zhu SH, Ding WN, Wu P, Yi KK (2012) OsGLU3, a putative membrane-bound endo-1,4-beta-glucanase, is required for root cell elongation and division in rice (*Oryza sativa* L.). Mol Plant 5:176–186. https://doi.org/10.1093/mp/ssr084.

Zhang P, Wu F, Kang X (2012) Genotypic variation in wood properties and growth traits of triploid hybrid clones of *Populus* tomentosa at three clonal trials. Tree Genet Genomes 8:1041–1050. https://doi.org/10.1007/s11295-012-0484-9.

Zhang R, Li B, Zhao Y, Zhu Y, Li L (2024) An essential role for mannan degradation in both cell growth and secondary cell wall formation. J Exp Bot 75:1407–1420. https://doi.org/10.1093/jxb/erad463.

Zhao Y, Song D, Sun J, Li L (2013) Populus endo-beta-mannanase PtrMAN6 plays a role in coordinating cell wall remodeling with suppression of secondary wall thickening through generation of oligosaccharide signals. Plant J 74:473–485. https://doi.org/10.1111/tpj.12137.

Zhao Y, Sun J, Xu P, Zhang R, Li L (2014) Intron-mediated alternative splicing of WOOD-ASSOCIATED NAC TRANSCRIPTION FACTOR1B regulates cell wall thickening during fiber development in *Populus* species. Plant Physiol 164:765–776. https://doi.org/10.1104/pp.113.231134.

Zhu Y, Li L (2021) Multi-layered regulation of plant cell wall thickening. Plant Cell Physiol 62:1867–1873. https://doi.org/10.1093/pcp/pcab152.

Zhu Y, Li L (2024) Wood of trees: cellular structure, molecular formation, and genetic engineering. J Integr Plant Biol 66:443–467. https://doi.org/10.1111/jipb.13589.

Zhu Y, Song D, Xu P, Sun J, Li L (2018) A HD-ZIP III gene, PtrHB4, is required for interfascicular cambium development in *Populus*. Plant Biotechnol J 16:808–817. https://doi.org/10.1111/pbi.12830.

Tree Physiology, 2025, tpaf051
https://doi.org/10.1093/treephys/tpaf051
Research paper